ISSN : 2321-9602

Indo-American Journal of Agricultural and Veterinary Sciences




editor@iajavs.com
iajavs.editor@gmail.com

Indo-Am. J. Agric. & Vet. Sci., 2022 *ISSN 2321–9602 www.iajavs.com*

Indo-American Journal of Agricultural and Veterinary Sciences

Vol. 10, Issuse 2, May 2022

A NOVEL ENHANCED LOW-RANK PRIOR FOR BLIND IMAGE DEBLURRING

B.PUSHPA LATHA,
ASSISTANT PROFESSOR DEPARTMENT OF ECE
DR.K.V.SUBBA REDDY INSTITUTE OF TECHNOLOGY, KURNOOL

ABSTRACT— Novel picture deconvolution algorithms separate the deblurring and denoising phases in a new way. As an example, in the deblurring stage, we use a regularised Fourier inversion to amplify or colourize noise, which corrupts the picture information. Specifically The coloured noise is effectively removed in the denoising stage using a singular-value decomposition of comparable packed patches. The threshold parameter may be updated at each iteration using a technique that updates the estimate of noise variance. In recent years, low-rank matrix approximation has been used to solve a variety of visual difficulties. For blind picture deblurring, we provide a new low-rank prior. An notable result from our study was the fact that even without employing any kernel information, a basic low-rank model may dramatically decrease blur in an input picture, while keeping essential edge information. The gradient map of a blurry input may be smoothed using the same model that was used to smooth out the input itself. Based on these characteristics, we present an upgraded prior for picture deblurring by merging the low rank prior of comparable patches from both the blurry image and its gradient map. By keeping the dominating edges and removing fine texture and faint edges from intermediate pictures, we are able to improve kernel estimation using a weighted nuclear norm minimization approach instead of a simple low-rank prior. For both uniform and nonuniform deblurring, we test the upgraded low-rank prior that has been presented. The experimental evaluations show that the proposed algorithm outperforms current deblurring approaches in both quantitative and qualitative terms.

Index Terms— Non-uniform deblurring, blind deblurring, low rank, weighted nuclear norm.

I. INTRODUCTION:

Out-of-focus photography or movements between objects and the camera during the exposure period may generate picture blur. Typically, the blur process is represented as follows:

b is equal to x k + n (1)

The observed blurry picture b is represented by the following equations: x = latent sharp image b + k + n + = convolution operator Picture deblurring is a problem in which the crisp latent image x is recovered from the fuzzy blurred image b. Non-blind image deblurring and blur kernel deblurring are both types of picture deblurring that may be used in conjunction with each other.

One and blind picture deblurring ([2, 3], respectively). For the blind image deblurring issue, the latent image x as well as the blur kernel K are unknown and must be

reconstructed given just the blurry picture b. It's a very bad issue to have, since the single viable solution is both unstable and non-unique.

For picture deblurring, the primary aim is to recover the latent image (l) and its related blur kernel (k). A lot of alternative combinations of the variables l and k may provide the same answer, making this a very bad issue to begin with. As a result, more information is needed for solution constrainedness. Prior knowledge from the statistics of natural images and blur kernels, such as heavy-tailed gradient distributions [1]–[3], normalised sparsity prior [4], sparsity constraints [5] and L0-regularized gradient [6], or a combination of both the intensity and gradient prior [7], is commonly used to solve this problem. The picture gradient is used to represent the interactions between pixel pairs in most of the aforementioned approaches. As real pictures are complicated in structure, it is challenging to simulate their more sophisticated structures using merely nearby pixels. This issue has been solved by various patch prior-based algorithms [8]–[13], which have achieved state of the art results in picture denoising and non-blind image deblurring. With the low-rank prior, picture denoising and nonblind deblurring have seen considerable gains in performance [12, 14]–[16] thanks to the low-rank prior.

In this study, we provide a new low-rank prior for blind picture deblurring that is more effective than previous methods (See Figure 1). As a result, we use the low-ranking characteristics of both

Image patches are used to create intensity and gradient maps. Using attributes of low rank, we reduce the weight of nuclear norm minimization to regularise the solution space of latent pictures. In addition, we offer a low rank prior for non-uniform picture deblurring, which we expand. [3] and [17] show that the proposed approach based on an upgraded low rank prior performs better than the current state-of-the art techniques for deblurring. The following is a list of the work's contributions: An technique for blind picture deblurring utilising low-rank matrix approximation has been proposed. A low-rank picture's intensity and gradient maps may be used to reconstruct the kernel estimation kernel's intermediate image for kernel estimation. While keeping dominating edges and fine texture features, the suggested low rank prior utilises an approach based on weighted nuclear norm reduction to improve the usefulness of low rank attributes even further. Non-uniform picture deblurring induced by camera rotation is addressed by extending the

(See Fig. 1): By using a low rank prior, it is possible to get more accurate estimates of the kernel.

The input seems to be a little hazy. (b) The final picture after using the method described above to remove blur. infrared spectra of (a). (2) on (c) without kernel estimate yields the following result: e) A graph showing the gradient of (a). Application of low rank model (2) to (e) without kernel estimation yields the following result in (f).

An existing system is referred to as "II."

To match the distribution of natural picture gradients, Fergus et al. use a combination of Gaussians, and variational Bayes inference is used to estimate the blur kernel. A new technique is presented by Shan et al.Natural photographs may be deblurred by concatenating two piece-wise continuous functions to suit the logarithmic gradient distribution. Levin et al. use a hyper-Laplacian

prior to describe the latent images and build an efficient marginal approximation approach to estimate blur kernels.

NEGATIVE FEATURES OF THE CURRENT SYSTEM

It takes a lot of time to query the external dataset. Kernel estimate is made more difficult by the high frequency hallucinations they produce, which aren't relevant for the process of estimating the kernel.

Relative Work and Problem Context III.

B**. Image Enhancement**

Image deblurring is separated into two types based on whether or not the blur kernel is known in advance. For decades, researchers have researched the non-blind image deblurring [1] method, which aims to recover a latent crisp picture with a known blur kernel. Due to the unstable nature of the inverse process and the fact that a tiny quantity of noise would cause large distortions, it is an ill-posed issue There are two well-known approaches to solving this problem: the Wiener filter and the Richardson-Lucy algorithm. Recently, the optimization issue of non-blind picture deblurring has been modelled. To cope with the ill-posedness in picture restoration, several well-known image priors, such as total variation (TV) [22] and sparse priors [17], [23], have been presented for regularisation. [2] and [3] blind image deblurring aims to restore a latently crisp picture without knowing the underlying blur kernel. [3] The use of gradient-based priors for natural photos is prone to failure, since they often prefer low-frequency images with a lot of blur. Many more complex priors, such as framelet-based priors [24], l0-norm-based priors [4], and priors that take into account the sparsity of the encoding, have been developed to address this issue, including low-rank priors [5], dark channel priors [6,] and others. Each, on the other hand, has flaws of its own. Handcrafted wavelet functions are at the heart of framelet-based priors [24], and as a result, they aren't flexible enough to handle a variety of blurring conditions. The convex relaxation to l1-norm of the l0-norm based prior [4] is sensitive parameter adjusting required for best performance since it is combinatorial in nature (therefore non-convex). A sparse-coding based prior presupposes that the training set and the target picture are statistically comparable, which may not be the case in fact. Solving the SVD problem for a low-rank prior [5] is expensive and time-consuming.

O(N3) as a whole. Complexity is another problem with the dark channel prior [6], which incorporates l0-norm and nonlinear dark channel computations. For the blind picture deblurring issue, we study the possibilities of graph-based priors. In a unique interpretation of RGTV as a graph l1-Laplacian regularizer, we provide a graph-based prior RGTV that is highly data-adaptive and easily solved utilising fast graph spectral filters.

A. Priors Based on the intensity of the image

Recently, picture patches for deblurring have been modelled using sparse representations [15]. To recover the latent picture, Hu et al. employ the sparsity constraints to learn an over-complete lexicon from a fuzzy image. Zhang et al. have suggested a new method for sparse representation.

Face recognition and deblurring may be done together [26]. When Cai et al. [5] create a technique for deblurring using wavelets, they ensure that both the crisp picture and blur kernel are subjected to sparsity restrictions [5]. Additionally, Couzinie-Devy et al. [27] use a linear mapping function to represent the clear and fuzzy picture patches and to develop a vocabulary to recover the crisp features that were lost. Multiple dictionaries are employed by Cao and colleagues [28] to characterise and deblur text pictures. Some areas may be resurrected using dictionary-based approaches, but they lack relevant information for kernel estimate and typically produce hallucinated high frequency material, which makes future kernel estimation more difficult [17].

B. Approximation Using a Low-Rank Matrix

Recently, low rank matrix approximation (LRMA) approaches have been developed and used to picture modelling. Numerous issues have been successfully tackled using the nuclear norm minimization (NNM) technique for LRMA, including robust principal component analysis

[29], visual tracking [30], matrix denoising [31], matrix completion [32], and low-level vision tasks [34]. Nonblind picture deblurring has also been tackled using the LRMA. Wang et al. [12] use a low rank based non-local spectral prior for non-blind picture deblurring. Gu et al. [16] recently presented a weighted nuclear norm minimization (WNNM) technique for picture denoising that allows for better adaptability and robustness. A weighting system for denoising is used in the WNNM technique [16], but we offer a new methodology to estimate weights particularly for deblurring. We use a low rank prior to eliminate fine texture from the intermediate photos in our technique. Kernel estimate relies heavily on the ability to discern fine features and microscopic edges in hazy pictures.

A. A Few Other, Non-Uniform Deblurring Techniques

According to Gupta et al. [35], for non-uniform deblurring, a 3D approximation that takes camera translation and in-plane rotation into account is the best solution. With state-of-the-art performance, a variety of methods have been created during the last several years. Using a low-dimensional subspace to constrain the various camera postures, Hu and Yang [39] offer an effective single picture deblurring approach that reduces computational overhead. Instead of employing the 6D transformation for camera motion, the approximate 3D models [35, 36] provide excellent results, as illustrated in [40]. Locally uniform approximation approaches have been developed in response to the computationally intensive nature of these methods.

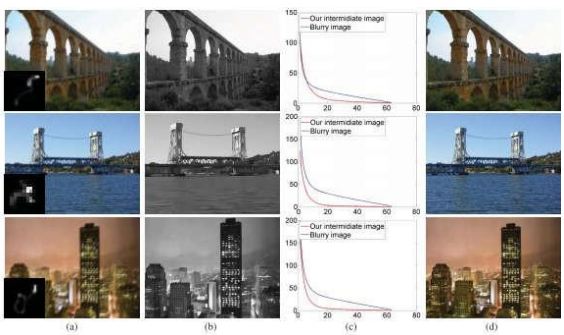

Fig2: Rank relationship between blurry and intermediate images. (a) Blurry inputs and kernels.
(a) Estimated intermediate pictures based on our technique. Non-local patches from (a) and (b) are shown in (c) with their average singular values. (d) The final findings after deblurring. Intermediary pictures have a lower non-local matrix rank than blurry ones.

INTRODUCTION TO ALGORITHM II

In Section V, we provide an efficient optimization approach for estimating blur kernels based on an LRMA model for blind picture deblurring. We begin by looking at the uniform situation, and then expand it to the non-uniform one.

A. Defining the Issue

With the MAP framework, we construct the deblurring issue. [Read more...] about

$$\{\hat{l}, \hat{k}\} = \arg\min_{l,k} p(l, k|b)$$
$$= \arg\min_{l,k} p(b|l, k)p(k)p(l),$$

The priors of the blur kernel and the latent image are p(k) and p(l), respectively. We use the minus log.

it is more likely that (3) and the suggested deblurring model

$$\{\hat{l}, \hat{k}\} = \arg\min_{l,k} \ell(l \otimes k, b) + \gamma\phi(k) + \lambda\varphi(l),$$

It's important that in this case, the recovered picture (l) be consistent with the observation (b), hence the first term in (4) refers to data fidelity. Its shape is determined by the noise model's predicted distribution. It is common practise for the fidelity function (lk, b) to penalise the discrepancy between l and b by using the 2-norm l k b2 2

20 and 44 through 46. Unlike l1-norm functions, these functions have been proven to be more sensitive to outliers [21]. A 1-norm data fidelity concept is used in this research. [21]

$$\ell(l \otimes k, b) = \|l \otimes k - b\|_1.$$

Kernel Prior: The second term is the constraint for the blur kernel, which is used to stabilize the solution of blur kernel k. In this paper, we use the l2- norm on blur kernel k,

$$\phi(k) = \|k\|_2^2,$$

The image previous is the last phrase in (4). Non-local surrounding patches on both intensity and gradient maps may be used for kernel estimation, as explained in Section III. The low rank qualities and sparse singular values are predicted when the non-local comparable patches are grouped into a matrix. Shrink the singular values in the LRMA process to eliminate noisy and fuzzy pixels, as seen in Figure 1(d) (f). Denoising [16], super resolution [47], non-blind deblurring [12], and picture restoration [48] are all examples of applications of the non-local self-similarity based approach. using a low rank prior based on the non-local selfsimilarity of both intensity and gradient patches

$$\varphi(I) = \sum_i \|I_i\|_* + \frac{\sigma}{\lambda} \sum_i \|\nabla I_i\|_*,$$

$$\varphi(I) = \sum_i \|I_i\|_{w,*} + \frac{\sigma}{\lambda} \sum_i \|\nabla I_i\|_{w,*}.$$

Algorithm 1 Deblurring by Enhanced Low Rank Prior

1: **Input**: Downsample the observed blurry image b to generate the image pyramid $\{b_0, b_1, \ldots, b_n\}$.
2: Estimate the blur kernels $\hat{k}_i$ and latent images $\hat{I}_i$ $(i = 1, 2, \ldots, n)$ in intermediate layers using [6] and output $\hat{k}_1$.
3: Upsample $\hat{k}_1$ to generate initial blur kernel k_0 for full resolution image b_0.
4: **for** $j = 1, 2, \ldots, 5$ **do**
5: solve d by minimizing (15).
6: $\beta \leftarrow 2\sigma$.
7: **repeat**
8: solve p by minimizing (16).
9: $\tau \leftarrow 2\lambda$.
10: **repeat**
11: solve g by minimizing (17).
12: solve l by minimizing (13).
13: $\tau \leftarrow 3\tau$.
14: **until** $\tau > \tau_{max}$.
15: $\beta \leftarrow 3\beta$.
16: **until** $\beta > \beta_{max}$
17: solve blur kernel k by (24).
18: $\lambda \leftarrow 0.9\lambda$, $\sigma \leftarrow 0.9\sigma$.
19: **end for**
20: With the final estimated kernel k, use the final deconvolution method [51] to generate the final output l.

II. LRMA FOR NON-UNIFORM DEBLURRING

The effects of camera shaking, including rotation and translation, tend to be spatially varied. It's common to think of it as,

$$\mathbf{b} = \sum_m k_m \mathbf{H}_m \mathbf{l} + \mathbf{n},$$

There are three vector forms for each of the three b, l and n vectors: There are two possible transformation matrices for each camera position, Hm and km. Hm is a rotation matrix, while km is a weighted average of the time spent in each camera stance. Note that the suggested low rank priors may be directly applied to MAP deblurring issues. It is possible to write this model of non-uniform deblurring as follows, using the MAP formulation (3).

$$\{\hat{I}, \hat{k}\} = \arg\min_{I,k} \|I \otimes k - b\|_1 + \gamma \|k\|_2^2 + \lambda \sum_i \|I_i\|_{w,*} + \sigma \sum_i \|\nabla I_i\|_{w,*}.$$

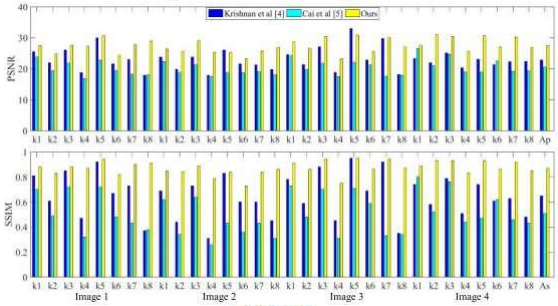

TABLE 1
IMAGE DEBLURRING RESULTS OF AVERAGE METRICS (PSNR, SSIM AND KS) USING DIFFERENT METHODS CORRESPONDING TO FIGURE 8

Average Metrics	PSNR	SSIM	KSIM
Krishnan *et al.* [4]	20.43	0.53	0.43
Cai *et al.* [5]	17.08	0.21	0.19
Zhong *et al.* [44]	18.33	0.49	0.28
Pan *et al.* [7]	14.51	0.16	0.54
Ours	**22.56**	**0.68**	**0.60**

Fig3: Quantitative evaluation in terms of PSNR and SSIM on the dataset [3]. The numbers below the horizontal axis denote the kernel and image index and the Ap and As on the rightmost columns denote the average PSNR and SSIM of all these images. Overall, the proposed algorithm performs favorably against the representative state-of-the-art methods

with priors based on image gradients and sparse representations

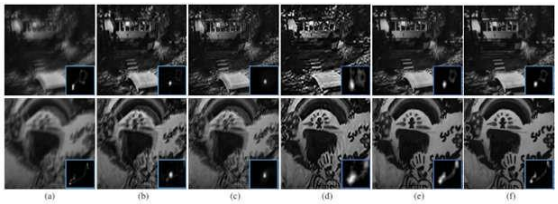

Fig4: Evaluation against representative methods with priors based on image gradients [4] and sparse representation Kernels and pictures that have been ground to a smeared texture (a) (2) Krishnan and coauthors (b). [4]. c) Cai and colleagues. [5]. D) Without the use of Li W,. Without 'li w,' we get these results. This is what we found.

INTERACTIVE EVALUATIONS

We compare the proposed approach to current state-of-the-art deblurring algorithms using both synthetic and actual photos in our studies. Kernel estimation and deblurred pictures are evaluated using a variety of measures including peak signal-to-noise ratios, structural similarity, kernel similarity, and cumulative error ratio distributions. We utilise the same settings in all of our experiments: = 5, = 0.05, = 1, max = 2 and max = 8. In photos with blur, we use 8 8 patches with a 1 pixel overlap between neighbouring patches. In a 30 30 pixel area, we use the block matching technique [16] to find patches that are comparable to each other.

Fig5: Visual comparison of state-of-the-art methods. These two blurry images in (a) are from [21]. (a) Blurry images. (b) Xu and Jia [21]. (c) Krishnan et al. [4]. (d) Xu et al. [6]. (e) Zhong et al. [44]. (f) Our results

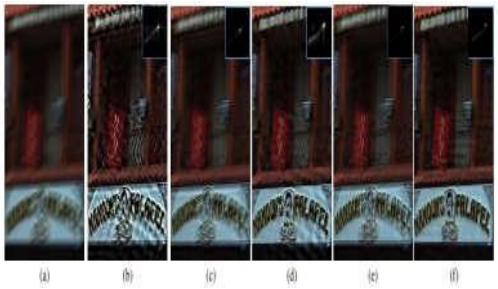

Fig6: In-depth visual comparison of cutting-edge research techniques. [44] is the source of the hazy picture in (a). a lack of clarity in the photographs. (3) Krishnan and colleagues [4] All rights reserved: (c) Xu et al. d) Zhong et al. f) Pan and colleagues [7]. This is what we found.

6.**1 Computer-Generated Images**

Using two datasets containing synthetically blurred photos, we compare the state-of-the-art deblurring approaches with the proposed methodology.

For the purpose of this study, we used the Levin et al. [3] dataset of 32 pictures created from four photographs and eight different kernels, and compared our technique against the best deblurring algorithms [1] through [7]. An example of the suggested method is shown in Figure 5a.

On this benchmark dataset, the cumulative error ratio of the low rank prior approach beats out the state-of-the-art methods. The PSNR and SSIM performance on each picture is shown in Figure 6, which compares two sample approaches that use priors based on image gradients and sparse representation [4], [5]. Figure 7 shows the outcomes of deblurring two photos from this dataset. If you look closely, you can see a few bright spots along the camera shaking trajectories in the kernels predicted by [4] and those estimated by [5]. Figures 7(d) and (e) illustrate the results using the proposed method without li w or liw, respectively, to help clarify the low rank priors of intensity and gradient. When the intensity previous li w, is omitted, the recovered pictures still have fuzzy borders, as seen in Figure 7(d). Figure 7(e) shows that the kernels calculated without utilising li w, are comparable to the ground truth, but may still be improved using the

gradient prior as in Figure 7 (f). As a result of this improvement, the proposed approach produces kernels that are more closely aligned with the actual data, resulting in cleaner recovered latent pictures.

Second, we use the dataset from Sun et al. [17] to conduct tests on hazy and noisy photos. It contains 640 pictures produced from 80 high-resolution nature photographs from a variety of settings and eight kernels. Each blurry picture also has a 1% Gaussian noise applied to it. On the left, you can see some of the estimated kernels and deblurred photos that were generated using the methodology described above and other current approaches. While the outputs from prior approaches have a lot of noise in them or are very near to delta functions [4], [5], the proposed methodology produces kernels that closely match the ground truth. Figure 8 shows the noisy estimated kernels and ringing artefacts in the [44] deblurred pictures (d). It is possible to deblur photos using the deblurring approach proposed by [7], although the final results include artefacts. Table I shows the average PSNR, SSIM, and KSIM values for each deblurred result for the photos presented in Figure 8 for each of the examined techniques

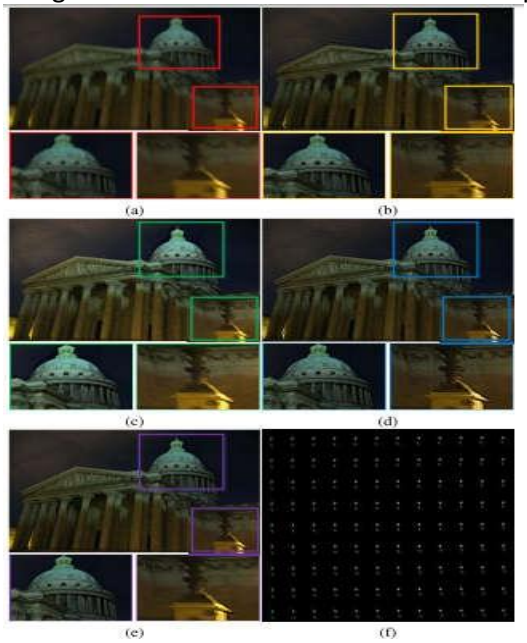

Fig7: Deblurring results of the Pantheon image with state-of-the-art non-uniform deblurring methods (best viewed on high-resolution display). (a) Blurry image.
(b) Whyte et al. [36]. (c) Hirsch et al. [43]. (d) Xu et al. [6]. (e) Our result. (f) Our estimated kernels

Fig8: Deblurring results of the Book image with state-of-the-art non-uniform deblurring methods (best viewed on high-resolution display). (a) Blurry image.
(b) Gupta et al. [35]. (c) Hu and Yang [39]. (d) Xu et al. [6]. (e) Our result. (f) Our estimated kernels.

III. CONCLUSIONS

A new low-rank prior for blind picture deblurring is presented in this study. The proposed approach takes use of the low-rank features of both intensity and gradient maps from picture patches. Weighted nuclear norm reduction based on low-rank qualities is used to recover latent pictures more successfully. Tests on benchmark datasets reveal that the proposed approach outperforms existing deblurring algorithms.

REFERENCES

[1] It was R. Fergus and B. Singh who published "Removing camera shaking from a single shot," in the ACM Transactions on

Graphics, volume 25, number 3, pages 787–794, in 2006.
[2] "High-quality motion deblurring from a single picture" was published by Q. Shan, J. Jia, and A. Agarwala in the journal ACM Trans. Graph., Vol. 27, No. 3, p. 73 in 2008.
[3] Understanding and assessing blind deconvolution methods are discussed at the IEEE Conference on Computer Vision and Pattern Recognition (CVPR) in June 2009, pp. 1964– 1971.
[4] A normalised sparsity measure for blind deconvolution was proposed by Dr. D. Krishnan, Tay, and Fergus, and published in the proceedings of the 2011 IEEE Conference on Computer Vision and Pattern Recognition.
[5] Framing-based blind motion de-blurring from a single picture has been proposed by a group of researchers, including Cai, Ji, Liu, and Shen.
[6] Unnatural L0 sparse representation for natural picture deblurring, by L. Xu, S. Zheng and J. Jia, in Proceedings of the 2013 IEEE Conference on Computer Vision and Pattern Recognition, pages 1107–1114.
[7] Deblurring text pictures with L0-regularized intensity and gradient prior, in Proceedings of the 2014 IEEE Conference on Computer Vision and Pattern Recognition, p. 2901–2908. [7]
[8] D. Zoran and Y. Weiss, "From learning models of natural picture patches to entire image restoration," in Proc. IEEE International Conference on Computer Vision, November 2011, pages 479–486, IEEE
[9] S. Roth and M. J. Black, "Fields of specialists," Int.
[10] In the April 2009 issue of J. Comput. Vis., volume 82, number 2, pages 205–229. 10 U. Schmidt, Q. Gao, and S. Roth, "A generative viewpoint on MRFs in low-level vision," in the IEEE Conference on Computer Vision and Pattern Recognition, June 2010, pages 1751–1758 [proc.].
[11] Non-local sparse models for image restoration" was published in the Proceedings of the IEEE 12th International Conference on Computer Vision in September/October 2009, pp. 2272–2279.
[12] Nonlocal spectral prior models for low-level vision are described in [12] by S. Wang, L. Zhang, and Y. Liang.
[13] For example, [13] W. Dong, L. Zhang, X. Wu, and G. Shi, "Image deblurring and super-resolution by adaptive sparse domain selection and adaptive regularisation," IEEE Transimage Processed 20(7):1838–1857, July 2011.
[14] A low-rank method to nonlocal picture restoration using bilateral variance estimation was published in the IEEE Transactions on Image Processing in 2013 in volume 22, number 2, pages 700–711.
[15] A nonlocally centralised sparse representation for picture restoration was published in IEEE Transactions on Image Processing in 2013, vol. 22, no. 4, pp. 1620–1630 (W. Dong et al., 2013).
[16] "Weighted nuclear norm minimization with an application to image denoising," in Proc. IEEE Conf. Comput. Vis. Pattern Recognit., June 2014, pp. 2862–2869.
[17] "Edge-based blur kernel estimate using patch priors," in IEEE Int. Conf. Comput. Photogr., April 2013, pp. 1–8. [17].
[18] "Efficient marginal likelihood optimization in blind deconvolution," by A Levin, Y Weiss, F. Durand, and W. T. Freeman, in Proc. IEEE Conf. Comput. Vis. Pattern Recognit.
[19] Blind deblurring via internal patch recurrence, by T. Michaeli and M. Irani, in Proc. 13th Eur. Conf. Computer Vis., 2014, pages 783–798, available online.
[20] p. 145, ACM Trans. Graph., vol. 28, no. 5, May 2009, S.
[21] L. Xu and J. Jia, "Two-phase kernel estimation for robust motion deblurring," in Proc. 11th Eur. Conf. Computer Vision, 2010, pp. 157–170 (in Chinese).
[22] For example, in the Proceedings of the 2014 European Conference on Computer Vision (ECCV), the authors of "Deblurring face photos using exemplars" describe how they used exemplars to "de-blur" face photographs.
[23] Deblurring by example using dense correspondence," in IEEE International

Conference on Computer Vision (ICCV), Dec. 2013, pp. 2384–2391.
[24] in Proc. of the 12th European Conference on Computer Visualization, pages 524–537 (2012), "Text picture deblurring utilising text-specific characteristics."